

Analysis of Oscillators with External Feedback Loop for Improved Locking Range and Noise Reduction

Heng-Chia Chang, *Member, IEEE*, Andrea Borgioli, Pochi Yeh, *Fellow, IEEE*, and Robert A. York, *Senior Member, IEEE*

Abstract—A simple scheme for enhancing the locking/capture range and phase-noise performance of FET-based voltage-controlled oscillators (VCO's) is presented using a low-pass feedback loop from the oscillator output to the varactor tuning port. The nonlinearity of the FET provides for mixer or phase detector behavior (a self-oscillating mixer). The resulting feedback oscillator advantageously combines the principles of a conventional injection-locked oscillator (ILO) and phase-locked loop (PLL), which we refer to as an injection-locked phase-locked loop (ILPLL). The analysis suggests that the ILPLL can be designed for superior near-carrier phase-noise performance compared with conventional ILO or PLL circuits. A 10-GHz prototype was fabricated, which demonstrated a locking range more than double that of the isolated VCO injection-locking range over the same range of injected signal power.

Index Terms—Feedback loop, injection-locked oscillator, injection-locked phase-locked loop, locking range, mixer, oscillator, phase detector, phase-locked loop, phase noise, transfer function, voltage-controlled oscillator.

I. INTRODUCTION

INJECTION locking of microwave oscillators [1] has been widely used for synchronization, high-gain amplification, and phasing of oscillators in communication electronics and phased-arrays. An injection-locked oscillator (ILO), shown in Fig. 1(a), is simply a conventional voltage-controlled oscillator (VCO) with some means for injecting an external RF signal. An ILO is a relatively simple circuit compared with alternative synchronization techniques such as phase-locked-loops (PLL's). However, ILO's have the disadvantage of a relatively small locking range compared with PLL's. The ILO locking range is related to the injection signal strength and the Q -factor of the oscillator intrinsic resonant circuit. Low Q -factors are required for wide locking range, but there are practical lower limits on the Q -factor relating to circuit realization and the necessity of maintaining oscillation at a desired frequency. Low- Q is also at odds with low phase noise, although this can be compensated near the carrier by the injection-locking process itself.

A standard PLL circuit uses a phase detector (PD), low-pass filter/amplifier, and a VCO. The gain and bandwidth of the loop determines the locking/capture range of the system; for most applications, this is a small fraction of the VCO center

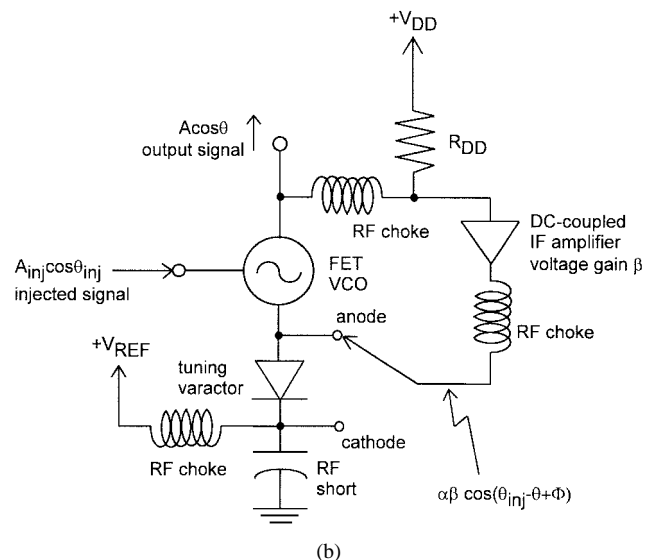
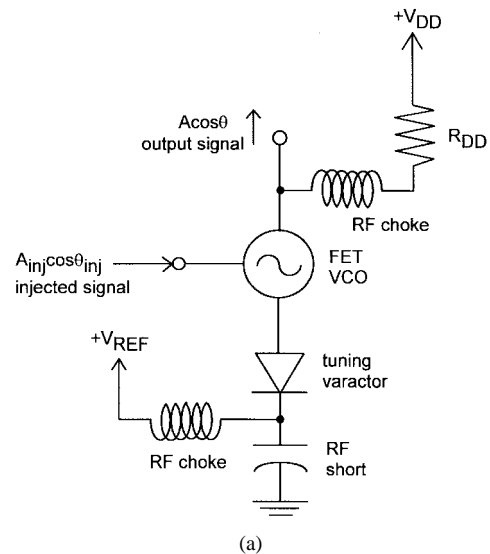


Fig. 1. (a) ILO with the injection port. (b) ILPLL where the VCO also serves as a PD, due to the inherent nonlinearity of the constituent devices. The dc amplifier output can be connected at the anode or cathode of the varactor diode. The connection position of the dc amplifier output can affect the locking bandwidth of the whole circuits.

frequency, although it can be much larger than the isolated VCO injection-locking range. Unlike the ILO, the locking range (or "hold-in" range) of a PLL can be easily controlled by adjusting the loop gain independent of the VCO characteristics. With proper design of the loop filter, near-carrier phase noise of the PLL can also be superior to an ILO.

Manuscript received November 20, 1997.

H.-C. Chang is with Santa Barbara Photonics Inc, Santa Barbara, CA 93111 USA.

A. Borgioli, P. Yeh, and R. A. York are with the Department of Electrical and Computer Engineering, University of California at Santa Barbara, Santa Barbara, CA 93106 USA (e-mail: ja@arctic.ece.ucsb.edu).

Publisher Item Identifier S 0018-9480(99)06092-5.

We recently proposed a simple circuit, which combines the principles of ILO and PLL in an efficient and advantageous manner, shown in Fig. 1(b). The circuit consists of a standard VCO with a low-frequency feedback loop connecting the VCO output to the varactor tuning port. This circuit makes use of the inherent nonlinearity of a VCO, which allows it to simultaneously provide the function of a mixer or PD, i.e., a self-oscillating mixer. As such, the circuit is similar to a PLL, where the PD and VCO functions are served by the same component. However, the following are two significant differences between this new circuit and a PLL; 1) since the external signal is directly injected into the VCO, the synchronization mechanism is a combination of ILO and PLL methods. For this reason, we label the circuit an injection-locked phase-locked loop (ILPLL) and 2) perhaps most significantly from an application standpoint, we show that, under certain conditions, the phase-noise characteristics of the ILPLL can be superior to both the ILO and PLL. Therefore, by simply adding a low-frequency dc-coupled amplifier to an existing VCO, we can create an oscillator with a potentially large locking range and exceptional phase-noise characteristics.

First-order phase dynamics of the ILPLL are first studied, assuming a FET-based VCO, in order to quantify the nonlinearity responsible for the mixing operation. The phase dynamics can be derived by extension of well-known injection-locking theory [1], leading to an equivalent Adler equation for the ILPLL. From this, it is shown that the locking range of the ILPLL can be larger than that of the ILO, by careful design of the phase shift and dc amplifier gain in the feedback loop. This is demonstrated and verified with a 10-GHz prototype circuit using a VCO based on a commercial packaged GaAs MESFET. We then present the amplitude dynamics, and then the theoretical results for the output phase noise, derived from the phase dynamics. No direct measurements of the phase noise or analysis of amplitude noise has yet been undertaken.

II. PHASE DYNAMICS AND LOCKING RANGE

When an oscillator is externally injected with a low-level RF signal, as depicted in Fig. 1(a), the phase dynamics of the ILO are described by [2]

$$\frac{d\theta}{dt} = \omega_o + \frac{\omega_o}{2Q} \operatorname{Im} \left\{ \frac{V_{\text{inj}}}{V} \right\} \quad (1)$$

where θ , ω_o , Q , and $V = A \exp(j\theta)$ are the instantaneous-phase free-running frequency (radian per second) Q -factor of the embedding network, and the phasor output voltage of the VCO, respectively. $V_{\text{inj}} = A_{\text{inj}} \exp(j\theta_{\text{inj}})$ is the phasor voltage associated with the injection signal. When the VCO is locked onto the injection signal

$$\frac{d\theta}{dt} = \omega_{\text{inj}} = \omega_o + \Delta\omega_{\text{lock}} \sin(\theta_{\text{inj}} - \theta) \quad (2)$$

where

$$\Delta\omega_{\text{lock}} = \frac{\omega_o}{2Q} \frac{A_{\text{inj}}}{A}.$$

We find that the oscillator can synchronize to an injected signal as long as

$$|\omega_{\text{inj}} - \omega_o| < \Delta\omega_{\text{lock}} \quad (3)$$

which indicates that $\Delta\omega_{\text{lock}}$ represents half the entire locking range.

Now consider the circuit of Fig. 1(b). If the frequency of the injected signal is such that (3) is not satisfied, then the oscillator *cannot* lock onto the injected signal; the nonlinearity of the oscillator will then generate mixing products. We can quantify this in a simple fashion assuming the I - V characteristics of an FET

$$I_{\text{ds}} = I_{\text{dss}} \left[1 - \frac{V_{\text{gs}}}{V_p} \right]^2 \quad (4)$$

where I_{dss} and V_p are the saturation current and pinchoff voltage of the MESFET, respectively. If the external signal is injected at the gate, then the gate voltage includes a contribution from both the oscillator and injected signal

$$V_{\text{gs}} = A'_{\text{vco}} \cos(\theta') + A_{\text{inj}} \cos(\theta_{\text{inj}}) \quad (5)$$

where A'_{vco} , θ' are the amplitude and phase of the intrinsic oscillator, measured at the gate (this would include pulling effects from the injected signal); A_{inj} , θ_{inj} are the amplitude and phase of the injection signal. Substituting (5) into (4) gives a low-frequency mixing product, which can be extracted from the drain through an RF choke and expressed as a voltage $\alpha \cos(\theta_{\text{inj}} - \theta')$, where

$$\alpha = - \frac{R_{\text{DD}} I_{\text{dss}} A'_{\text{vco}} A_{\text{inj}}}{V_p^2} \quad (6)$$

and where R_{DD} is the drain bias resistor, as shown in Fig. 1(b). This low-frequency signal is then amplified and fed back to the varactor bias network, as in a PLL. The output of the dc amplifier is expressed as $\alpha\beta \cos(\theta_{\text{inj}} - \theta + \Phi)$, where β is the loop amplifier voltage gain and Φ is a phase term that includes the phase shift from gate to drain through the device, and any residual phase shift around the loop. This could be determined empirically if accurate nonlinear models are not available for the device.

The intrinsic VCO frequency will track the low-frequency voltage on the varactor such that

$$\omega_o = \omega' \pm \beta\alpha K_0 \cos(\theta_{\text{inj}} - \theta + \Phi) \quad (7)$$

where ω' is the VCO frequency with the feedback loop and injection source removed, and K_0 is the tuning sensitivity of the VCO with units of radians per second per volt. The “ \pm ” sign in (7) refers to whether the amplifier output is connected to the cathode or anode side of the varactor, as shown in Fig. 1(b). Substituting (7) into (2) and assuming that $\alpha\beta K_0 \ll \omega'$ gives a new phase equation

$$\frac{d\theta}{dt} = \omega' + \Delta\omega_{\text{lock}} \sin(\theta_{\text{inj}} - \theta) \pm \alpha\beta K_0 \cos(\theta_{\text{inj}} - \theta + \Phi). \quad (8)$$

Comparing (8) with (1) shows that we can view the circuit as an ILO with two injection signals, one due to the external

source, and the second coming from the feedback loop. These terms can be combined using trigonometric identities into an equivalent Adler equation for the circuit

$$\frac{d\theta}{dt} = \omega_{\text{inj}} = \omega' + \Delta\omega'_{\text{lock}} \sin(\theta_{\text{inj}} - \theta + \Phi') \quad (9)$$

where

$$\Delta\omega'_{\text{lock}} = \sqrt{(\alpha\beta K_0)^2 + (\Delta\omega_{\text{lock}})^2 \mp 2\alpha\beta K_0 \Delta\omega_{\text{lock}} \sin \Phi} \quad (10)$$

and

$$\Phi' = \tan^{-1} \left[\frac{\alpha\beta K_0 \cos \Phi}{\Delta\omega_{\text{lock}} \mp \alpha\beta K_0 \sin \Phi} \right]. \quad (11)$$

The upper sign in the above equations is for the dc amplifier output connected at the cathode of the varactor, and the lower sign is for the anode of the varactor. Clearly, $\Delta\omega'_{\text{lock}}$ can be regarded as the new locking range of the system, and can be increased. Note that a measurement of locking range for the case of no feedback and the two different methods for connecting to the varactor give sufficient information to uniquely determine all of the required parameters in the model.

In order to insure that the locking range of the ILPLL is larger than that of the ILO or $\Delta\omega'_{\text{lock}} > \Delta\omega_{\text{lock}}$, we must have

$$\beta > \pm \frac{2\Delta\omega_{\text{lock}}}{\alpha K_0} \sin \Phi. \quad (12)$$

This shows that, for any given Φ , we can always obtain an increase in the locking range by either adjusting the point of feedback on the varactor or by using an inverting or noninverting amplifier. Clearly, it is important to characterize the parameter Φ . Once done, the locking range can then be increased easily by increasing R_{DD} or increasing the loop gain β . Also note that we have ignored the effects of loop filtering in this first-order analysis. These conclusions will apply without significant modification as long as the loop bandwidth equals or exceeds the desired locking bandwidth.

III. AMPLITUDE DYNAMICS

As the oscillator is injected by an external signal, the amplitude-dynamics equation of the ILO is [1], [2]

$$\frac{dA}{dt} = \mu \frac{\omega_0}{2Q} A(A_0^2 - A^2) + \frac{\omega_0}{2Q} A \cdot \text{Re} \left\{ \frac{V_{\text{inj}}}{V} \right\} \quad (13)$$

where A , μ , A_0 , and Q are the output voltage amplitude after locking, the gain saturation parameter, the free-running output voltage amplitude, and Q -factor, respectively. For the ILPLL, the output of the dc amplifier is $\alpha\beta \cdot \exp[j(\theta - \theta_{\text{inj}} + \Phi)]$. Therefore, the normalized total injection voltage phasor of the oscillator V_{inj}/V becomes

$$\frac{V_{\text{inj}}}{V} = \frac{\alpha\beta}{A} e^{j(\theta - \theta_{\text{inj}} + \Phi)} + \frac{A_{\text{inj}}}{A} e^{j(\theta_{\text{inj}} - \theta)} \quad (14)$$

and the amplitude dynamics of the ILPLL is

$$\frac{dA}{dt} = \mu \frac{\omega_0}{2Q} A(A_0^2 - A^2) + \frac{\omega_0}{2Q} \alpha\beta \cos(\theta - \theta_{\text{inj}} + \Phi) + \frac{\omega_0}{2Q} A_{\text{inj}} \cos(\theta_{\text{inj}} - \theta). \quad (15)$$

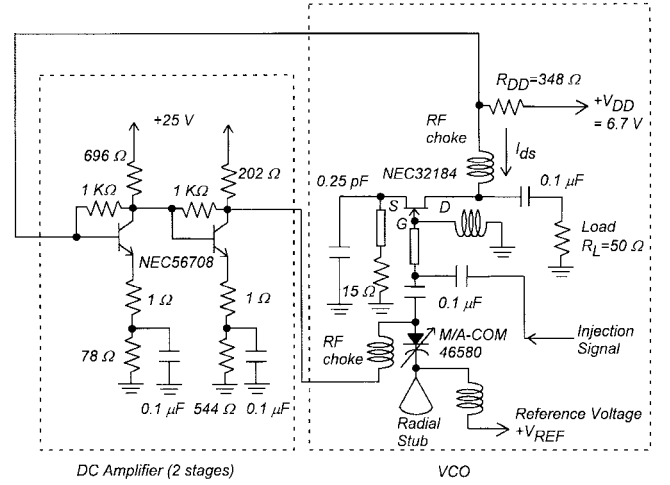


Fig. 2. The prototype circuit used in this paper. The VCO is designed as a common-gate GaAs MESFET circuit operating at 10 GHz. The feedback amplifier is a simple dc-coupled two-staged BJT design with over 30-dBm voltage gain for broad input frequency range. The measured characteristics of the whole ILPLL are dependent on the dc amplifier output connection position to the varactor diode.

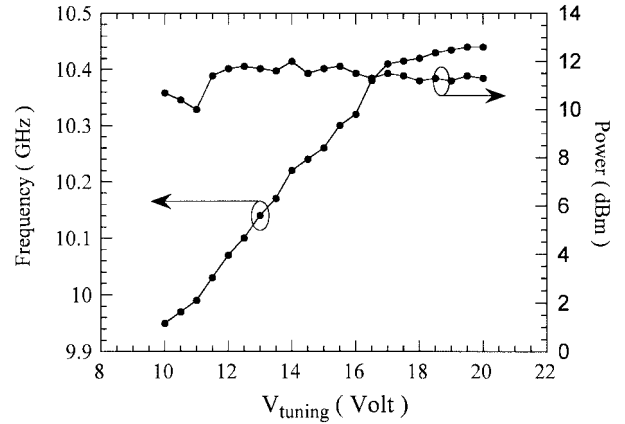


Fig. 3. The tuning range and output power of one single free-running VCO (without feedback loop) versus the tuning voltage.

The locking bandwidth of the oscillator is affected by the connection of the dc amplifier output at the anode or cathode of the varactor diode. However, the amplitude dynamics of the oscillator in the ILPLL is not affected by the connection position of the dc amplifier output at the cathode or anode of the varactor diode.

IV. EXPERIMENTAL RESULTS

The ILPLL concept was verified using a 10-GHz prototype circuit [4]. The VCO was designed with an NEC32184A GaAs MESFET in a common gate configuration for a large tuning range, and uses an M/A-COM 46580 beam-lead hyperabrupt varactor diode (Fig. 2). The tuning range and output power versus the tuning voltage of the VCO component are shown in Fig. 3. From this figure, we can determine the tuning sensitivity as $K_0 \simeq 63$ MHz/V in the linear region. The external signal is injected from an HP 8350B sweep oscillator at the gate through a one-wavelength 50- Ω microstrip transmission line. As described earlier, the nonlinearity of the FET will mix

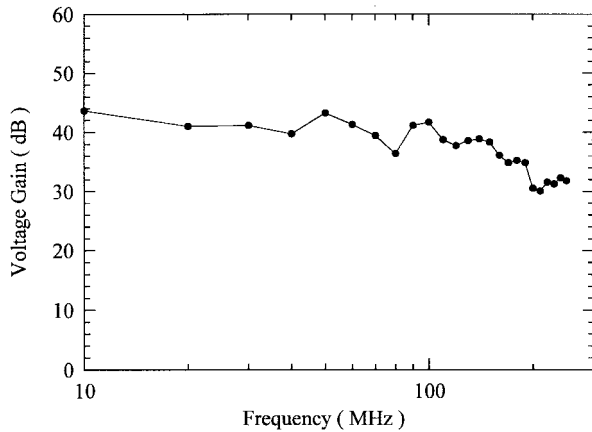


Fig. 4. The voltage gain of the two-staged dc BJT amplifier versus the input signal frequency.

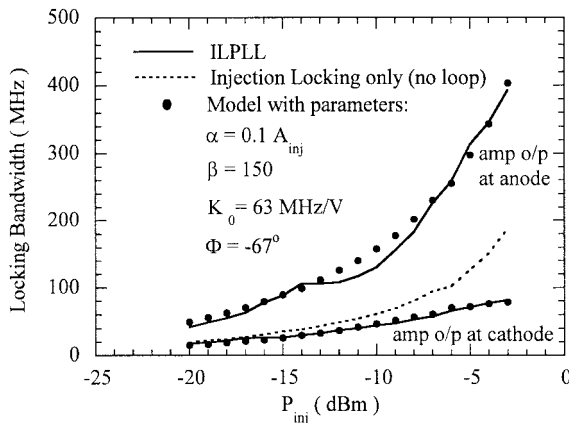


Fig. 5. The experimental results and the models of the locking bandwidth of the ILPLL for different connection positions of dc amplifier output at the varactor diode. The models are quite consistent with the experimental results.

the oscillator signal against the injection signal, and the mixing product will be superimposed on the oscillator output. The RF choke used in the bias circuit serves as a low-pass filter, coupling the low-frequency mixing products to an amplifier. The output of the amplifier is, in turn, fed back to the varactor through a second RF choke. The varactor diode cathode is biased with a reference voltage at a virtual RF ground, with the anode end connected to the FET gate, which is also a dc ground via an RF choke. The low-frequency feedback can then be introduced at either the cathode or anode end, which changes the sign of the feedback signal on the FET gate.

The loop amplifier uses a two-stage bipolar junction transistor (BJT) (NEC56708) broad-band feedback amplifier [5], which provides over 30 dB of gain up to 300 MHz, with a linear gain near dc of approximately $\beta \approx 150$. The frequency response of the amplifier is shown in Fig. 4. The low-frequency gain of the amplifier is of most interest for the “hold-in” range, while the bandwidth of the loop strongly influences the “capture” range of the system.

The measured locking ranges for the isolated VCO (ILO) and the ILPLL for both possible varactor configurations are shown in Fig. 5. The locking range in this figure is the

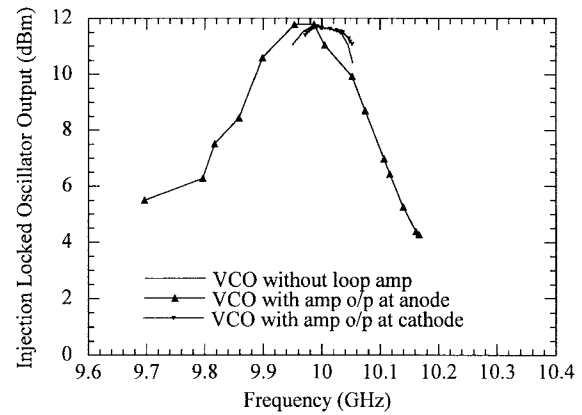


Fig. 6. The experimental results of the output power of the ILPLL system for different connection positions of dc amplifier output at the varactor diode under external injection power $P_{inj} = -3.0$ dBm. The output power (or amplitude dynamics) of the whole system is not affected by the connection position of the dc amplifier output, but the locking bandwidth of the system is affected.

full locking range, i.e., $2\Delta\omega_{lock}$. The figure clearly shows that the locking ranges can be significantly improved by the feedback amplifier; in this case, when the dc amplifier output is connected at the anode of the varactor diode. This ILPLL, therefore, has $\sin \Phi < 0$. The locking range for the ILPLL is more than doubled over the range of injection power examined compared with the ILO. This is a significant improvement for coupled oscillator applications [2], [3], [7], [10], [11]. Note that the *increase* in the locking range is not simply a loading effect whereby the loop amplifier decreases the Q -factor of the VCO; this is verified by the *decrease* in the locking range when the amplifier is connected at the cathode of the varactor. The locking range could be further increased by increasing the gain of the feedback amplifier or the drain resistor R_{DD} . In addition, the circuit could be improved significantly by providing a matching network for the injection source.

Using the model (10), we find an excellent fit to the measured data using the measured amplifier and VCO characteristics along with best-fit parameters $\alpha = 0.1A_{inj}$ and $\Phi \approx -67^\circ$, where A_{inj} is the external injection source voltage amplitude (estimated from the known injection power and an assumed load impedance). The model predictions are shown as solid dots in Fig. 5.

The measured output power versus injection frequency for the ILPLL is shown in Fig. 6, over the range of frequencies associated with the respective locking ranges for each case. The ILO amplitude variation is also shown. In all the measurements, an injection power of -3 dBm was used. The amplitude variation for the ILO case is related primarily to the saturation of the device nonlinearity, whereas for the ILPLL case with enhanced locking range, the amplitude variation also includes a large contribution due to the frequency dependence of the nonlinearity, which we can think of as an equivalent frequency-dependent negative resistance. It is possible to improve the circuit design to minimize the variation in equivalent negative resistance versus frequency and, thus, “flatten” out the amplitude variation. This has not yet been attempted.

V. NOISE ANALYSIS

In this section, we will find the upper and lower bounds of the phase noise of our ILPLL, and the conventional PLL for comparison. In the simulations, we assume that the phase noise of the dc amplifier introduced in the ILPLL is very small and negligible as compared to that of the oscillator or PD. For the best case, we assume that the phase noise of the PD is zero. As a worst case, we assume that the phase noise introduced by the PD is the same as that of the oscillator in the system for calculation convenience.

To analyze the output phase noise of the ILPLL, a noise admittance is used to represent the internal noise source of the oscillator [6], [8]–[10], and a loop transfer function [12]–[14] to describe the circuit external to the VCO. The approach involves linearizing the system under the assumption of small fluctuations, and transform to the frequency domain to examine the spectral characteristics of the noise. In this analysis, we neglect AM noise and possible AM-to-PM conversion in the VCO; therefore, the analytical results are expected to be optimistic and are primarily intended to compare the ILPLL scheme with the ILO and PLL.

Under these assumption, it has been shown that the output phase noise of a single ILO is [6], [8]–[10]

$$|\tilde{\delta\theta}_{\text{osc}}|^2 = \frac{\left(\frac{\omega}{\omega_{3\text{dB}}}\right)^2 |\tilde{\delta\theta}_0|^2}{\left(\frac{\omega}{\omega_{3\text{dB}}}\right)^2 + \rho^2 \cos^2(\hat{\theta} - \hat{\theta}_{\text{inj}})} + \frac{\rho^2 \cos^2(\hat{\theta} - \hat{\theta}_{\text{inj}}) |\tilde{\delta\theta}_{\text{inj}}|^2}{\left(\frac{\omega}{\omega_{3\text{dB}}}\right)^2 + \rho^2 \cos^2(\hat{\theta} - \hat{\theta}_{\text{inj}})} \quad (16)$$

where the tilde ($\tilde{\cdot}$) denotes a transformed or spectral variable, ω is the frequency offset from the carrier, $\omega_{3\text{dB}} = \omega_0/(2Q)$ is the full-width-half-maximum bandwidth of the free-running oscillator's embedding circuit (i.e., the 3-dB bandwidth), and ω_0 is the free-running frequency of the slaved oscillator. $\rho = A_{\text{inj}}/A$ is the relative injection signal amplitude normalized to the free-running signal amplitude, $\hat{\theta}$ is the steady-state value of the output phase, and $\hat{\theta}_{\text{inj}}$ is the injection signal phase. $|\tilde{\delta\theta}_0|^2$ represents the power spectral density of the phase noise of the free-running oscillator, and $|\tilde{\delta\theta}_{\text{inj}}|^2$ is, similarly, the phase noise of the injection signal into the oscillator [6], [8]–[10]. From (16), the ILO phase noise is that of the injection source near carrier frequency, and returns to its free-running noise for the noise offset frequency far from the carrier frequency.

A similar analytical approach is applied to the ILPLL using the block diagram in Fig. 7 [12]–[14]. In this figure, K_0 is the slaved oscillator transfer function (the tuning sensitivity), $K_d \equiv \alpha$ is the PD transfer function linearized around the operating point (PD sensitivity), and $F(\omega)$ is the transfer function of the dc amplifier and associated filtering components. These transfer functions are used to examine how the spectral characteristics of noise are affected by the feedback. The noise associated with each block function is linearly superimposed with the signal immediately following the transfer function. $\tilde{\delta\theta}_{\text{osc}}$ is the output phase fluctuation of the ILO as given by (16), $\tilde{\delta\Omega}_d$ is the noise introduced by the PD, and $\tilde{\delta\Omega}_a$ is the dc amplifier noise (different symbols are used for the PD and amplifier noise since these are amplitude fluctuations). The

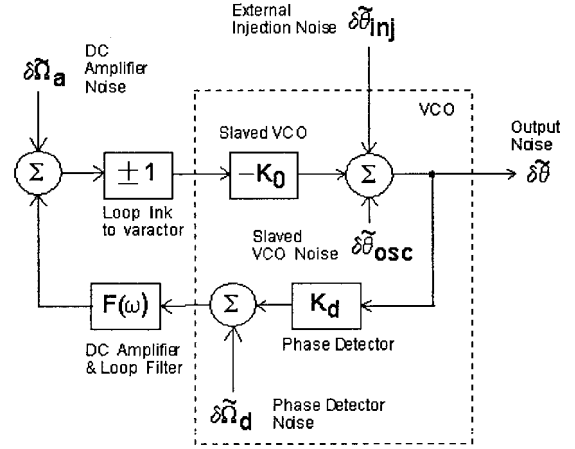


Fig. 7. The block diagram of the ILPLL system. The noise introduced by each transfer function can be added with the respective output signal for the calculation of total output noise power spectral density of the system. The VCO can also act as the PD (or mixer) function, and the noise of the slaved oscillator and that of the PD function may be correlated. The block diagram of “ ± 1 ” in the ILPLL represents the effects of the dc amplifier output connection position at the varactor diode on the ILPLL performances. The “ $+1$ ” means the amplifier output connected at the cathode and “ -1 ” at the anode of the varactor diode.

output phase fluctuation is easily found as

$$\tilde{\delta\theta} = \frac{\tilde{\delta\theta}_{\text{osc}} \pm K_0(\tilde{\delta\Omega}_a + \tilde{\delta\Omega}_d F(\omega)) \pm K_0 K_d F(\omega) \tilde{\delta\theta}_{\text{inj}}}{1 \pm K_0 K_d F(\omega)} \quad (17)$$

The power spectral density of the output noise is then found as $\langle |\tilde{\delta\theta}^* \tilde{\delta\theta}| \rangle$, where $\langle \cdot \rangle$ denotes an ensemble average (this notation is subsequently suppressed). Computation of the power spectral density, therefore, requires knowledge of the cross correlation of all the various noise sources in Fig. 7. Since the VCO is functioning as both an ILO and PD, the phase fluctuations $\tilde{\delta\theta}_{\text{osc}}$ and $\tilde{\delta\Omega}_d$ are probably correlated to some extent; a noise correlation coefficient C_n is used to express this correlation as

$$\left| \frac{\tilde{\delta\Omega}_d}{K_d} \cdot \tilde{\delta\theta}_{\text{osc}}^* \right| = C_n |\tilde{\delta\theta}_{\text{osc}}|^2$$

where $0 \leq C_n \leq 1$. We assume all other noise sources are uncorrelated. The output phase noise of the ILPLL circuit then becomes

$$\begin{aligned} |\tilde{\delta\theta}|^2 &= |1 - H(\omega)|^2 |\tilde{\delta\theta}_{\text{osc}}|^2 + |H(\omega)|^2 \left| \frac{\tilde{\delta\Omega}_d}{K_d} \right|^2 \\ &\pm \frac{(F(\omega) + F^*(\omega)) K_d K_0}{|1 \pm F(\omega) K_d K_0|^2} C_n |\tilde{\delta\theta}_{\text{osc}}|^2 \\ &+ \frac{|K_0|^2}{|1 \pm F(\omega) K_d K_0|^2} |\tilde{\delta\Omega}_a|^2 \end{aligned} \quad (18)$$

where the loop transfer function is

$$H(\omega) = \frac{\pm F(\omega) K_d K_0}{1 \pm F(\omega) K_d K_0} \quad (19)$$

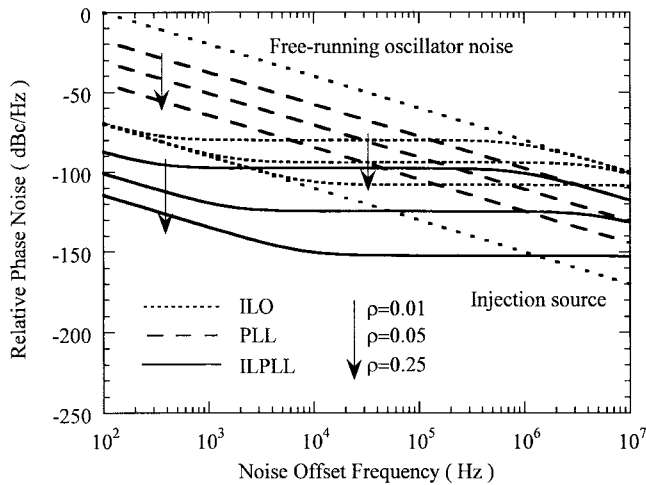


Fig. 8. Spectral characteristics of the relative output phase noise of the free-running oscillator, external injection source, ILO (with feedback loop), conventional PLL, and ILPLL with the first-order loop versus normalized injection source strength ρ . The phase-noise curves of PLL and ILPLL shown here use the assumption that PD noise in the circuits is zero for best case. The ILPLL has lower output phase noise than the PLL in the low-noise offset frequency range for the best case.

From (7), the upper sign is for feedback to the varactor cathode, and the lower sign is for anode connection. The spectral characteristics of the output noise are, therefore, strongly dependent on the filter function $F(\omega)$. In the following, we discuss two loop transfer functions: a first-order loop and a second-order loop.

A. First-Order Loop

A first-order low-pass loop transfer function is [12]–[14]

$$F(\omega) = F_1(\omega) = \frac{G}{1 + j\omega T_0} \quad (20)$$

where $1/T_0$ is the dominant pole of the loop transfer function. This is a good approximation for our prototype circuit using the parameters $G = 100$, and $T_0 = 2.386 \times 10^{-9}$. Substituting (20) into (18) and using the model parameters previously described allow us to compute the expected noise spectral characteristics for a given set of noise sources. For the purposes of illustration, we assume that the injected signal and free-running noise sources have ideal $1/\omega^2$ dependence, with an injected signal noise several orders of magnitude lower (better) than the free-running FET oscillator. We also assume that the contribution to output noise due to fluctuations in the loop amplifier ($\delta\Omega_a$) are negligible in comparison to those of the oscillator and phase detector.

With the above transfer functions, we plot the phase-noise curves of the free-running oscillator, injection source, ILO without feedback loop, PLL, and ILPLL with different normalized injection source strength (Fig. 8). The PLL use the same PD and amplifier (or filter) transfer functions as those in the ILPLL, but the VCO phase noise in the PLL is independent of an external injection source. We have assumed that the output steady-state phase of the oscillator is the same

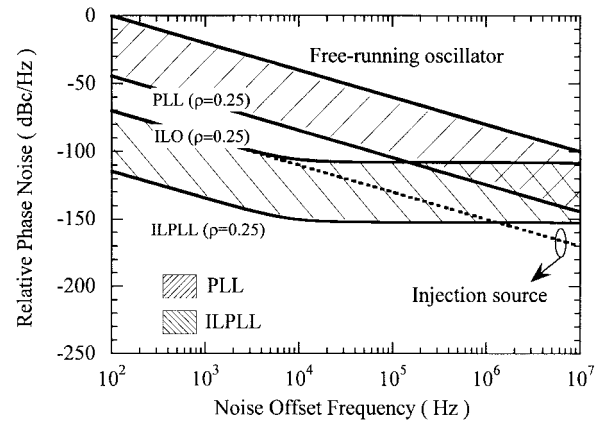


Fig. 9. Spectral characteristics of the relative output phase noise of the ILO (without feedback loop), conventional PLL, and ILPLL with the first-order loop at normalized injection source strength $\rho = 0.25$. The possible output phase-noise ranges of the ILPLL and conventional PLL are also shown in the figure, which are affected by the magnitude of the phase detector (or the mixer) noise in the circuits (see text).

as that of the external injection source for simplicity (i.e., $\hat{\theta} = \hat{\theta}_{inj}$), and the PD noise in the ILPLL or PLL is zero for the best case (or lower bound). We find the output phase noise of the ILPLL with zero PD noise can be much lower than that of the PLL with same conditions at low-noise offset frequency. The noise reduction at low-noise offset frequency is due to the dc amplifier transfer function in the feedback loop, which can reduce the output sensitivity and phase noise of the whole ILPLL feedback system. For higher injection strength ρ , the phase noise of ILO improves further [8], and that of the ILPLL also improves. From (9) to (11), we know that the phase dynamics equation, new locking bandwidth $\Delta\omega'_{lock}$, and the new phase Φ' depend on the connection position of the dc amplifier output at the cathode or anode of the varactor diode. The simulation results show that the output phase-noise curves of the system for different connection positions of the dc amplifier output at the varactor diode are virtually indistinguishable from each other and, thus, difficult to present on the same curve for comparison (Fig. 8). The cross-correlation noise term between the ILO noise and PD noise in the ILPLL is also very small and can be neglected.

In Fig. 9, the possible phase-noise ranges for ILPLL and PLL are shown for comparison. In the best case of the ILPLL, where the PD noise in the ILO is zero, the output phase noise of the ILPLL can be much lower than the conventional PLL with zero PD noise. In the worst case of the ILPLL, where the PD noise in the oscillator device has same noise power spectral density as the ILO, the output phase noise of the ILPLL tracks the noise curve of the ILO without any loop. In the best case of the PLL where the PD noise is zero, the phase-noise curve is very small over a broad noise offset frequency range. In the worst case of the PLL, where the PD noise power spectral density is the same as the oscillator noise, the output phase of the PLL tracks the noise curve of the free-running oscillator. Therefore, we find the upper and lower bounds of the possible phase noise for the ILPLL and PLL. For clarity of the figures, we only plot the case of $\rho = 0.25$ in Fig. 9 to show the possible phase-noise ranges of our ILPLL and the conventional PLL.

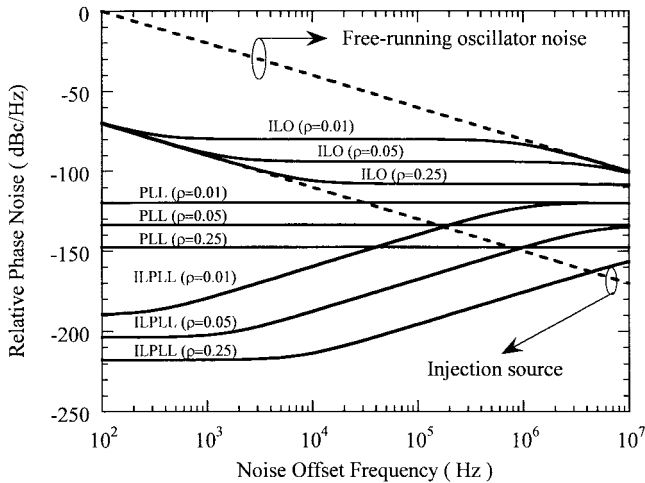


Fig. 10. Spectral characteristics of the relative output phase noise of the free-running oscillator, external injection source, ILO (without feedback loop), conventional PLL, and ILPLL with the second-order loop versus normalized injection source strength ρ . The phase-noise curves of PLL and ILPLL shown here use the assumption that PD noise in the circuits is zero for the best case. The ILPLL has lower output phase noise than PLL in the low-noise offset frequency range for the best case.

B. Second-Order Loop

The transfer function $F(\omega)$ of the dc amplifier (or the combined dc amplifier and low-pass filter) for a second-order loop [12]–[14] is

$$F(\omega) = F_2(\omega) = \frac{j\omega T_2 + 1}{j\omega T_1} \quad (21)$$

where T_1 and T_2 are the parameters of the dc amplifier. We can use the measured parameters of our prototype ILPLL at 10 GHz in the noise simulations. We can design the dc amplifier with the parameters $T_1 = 1.0848 \cdot 10^{-10}$ second and $T_2 = 3.389 \cdot 10^{-9}$ second to obtain 30 dBm of the power gain of the loop dc amplifier over a large input frequency range. The VCO tuning sensitivity is assumed $K_0 = 63$ MHz/V, and the PD function of the VCO is $K_d = 0.1A_{inj}$ with the unit of volts per megahertz, where A_{inj} is the amplitude of the external injection signal with the unit of volt.

With the above transfer functions, we can plot the phase-noise curves of the free-running oscillator, injection source, ILO without feedback loop, PLL, and ILPLL with different normalized injection source strength (Fig. 10). The PLL uses the same PD and amplifier (or filter) transfer functions as those in the ILPLL, but the VCO phase noise in the PLL is independent of an external injection source. We have assumed that the output steady-state phase of the oscillator is the same as that of the external injection source for simplicity (i.e., $\hat{\theta} = \hat{\theta}_{inj}$), and the PD noise in the ILPLL or PLL is zero for the best case (or lower bound). We find the output phase noise of the ILPLL with the second-order loop has much better noise reduction than the one with the first-order loop. The phase noise of the PLL with the second-order loop also has lower phase noise than the one with the first-order loop.

In Fig. 11, the possible phase-noise ranges for the ILPLL and PLL are shown for comparison. In the best case of the ILPLL, where the PD noise in the ILO is zero, the output phase

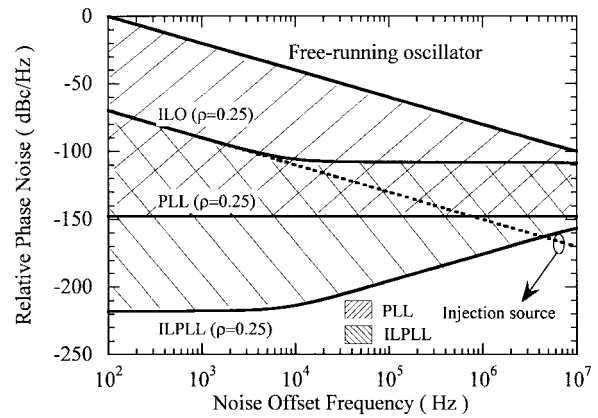


Fig. 11. Spectral characteristics of the relative output phase noise of the ILO (without feedback loop), conventional PLL, and ILPLL with the second-order loop at normalized injection source strength $\rho = 0.25$. The possible output phase-noise ranges of the ILPLL and conventional PLL are also shown, which are affected by the magnitude of the phase detector (or the mixer) noise in the circuits (see text).

noise of the ILPLL can be much lower than the conventional PLL with zero PD noise. In the worst case of the ILPLL, where the PD noise in the oscillator device has the same noise power spectral density as the ILO, the output phase noise of the ILPLL tracks the noise curve of the ILO without any loop. In the best case of the PLL, where the PD noise is zero, the phase-noise curve is very small over a broad noise offset frequency range. In the worst case of the PLL, where the PD noise power spectral density is same as the oscillator noise, the output phase of the PLL tracks the noise curve of the free-running oscillator. Therefore, we find the upper and lower bounds of the possible phase noise for the ILPLL and PLL. For clarity of the figures, we only plot the case of $\rho = 0.25$ in Fig. 11 to show the possible phase-noise ranges of our ILPLL and the conventional PLL.

In the above simulations, we study the first- and second-order loop for our ILPLL. The ILPLL with the second-order loop can have much better output phase-noise reduction than the one with first-order loop. However, in reality, the first-order loop is much easier to implement than the second-order loop because the typical dc amplifier belongs to the first-order loop. It should be noted that the curves in Figs. 8–11 only consider the contributions of the oscillator phase-noise sources. The phase-noise relation of the ILO and PD function inside the ILPLL is not well known. In the simulations, we also neglect the background thermal noise introduced by the resistors in ILPLL circuits, dc amplifier noise, oscillator AM noise and AM-to-PM noise conversion, and PM noise deterioration due to the nonzero steady-state phase difference between the oscillator output and injection source [6], [8]. Unfortunately, it is very complicated to completely treat the whole output phase noise of the ILPLL. However, it is possible to minimize these effects by careful design of the low-noise oscillator in the ILPLL in order to reach the lower bound curve as closely as possible.

VI. CONCLUSION

We have extended the previous reported work [4] of a simple scheme for enhancing the hold-in and capture ranges of

standard MESFET VCO's using an inexpensive low-frequency dc-coupled feedback amplifier which combines the injection-locked and PLL methods. Such a circuit can be termed an ILPLL since injection-locked and PLL processes are at work. The oscillator in the ILPLL also provides the function of a mixer or PD. In this paper, we investigate the phase and amplitude dynamics of the ILPLL. The locking range of the ILPLL can be more than double that of the isolated VCO injection-locking range over the same range of injected signal power. The amplitude dynamics of the ILPLL is not affected by the connection position of dc amplifier output at the anode or cathode of the varactor diode. These theoretical predictions are consistent with our experimental results. We also propose a simple method to analyze the phase noise of the ILPLL to compare the phase-noise performance with the free-running oscillator, external injection signal, ILO without any feedback loop, and conventional PLL. The output phase noise of the ILPLL combines the properties of the ILO and PLL, and has exceptional noise reduction at low-noise offset frequencies, where we have assumed that the noise of the PD function of the oscillator is much smaller than the oscillator phase noise.

By careful design of the oscillator and the loop transfer function, we can improve the output phase noise at low-noise offset frequency of the ILPLL. Such circuit design of ILPLL combining the injection locking and PLL is cheap, easy to design, and can be applied to any frequency range because no PD (or mixer) design is involved. The ILPLL can be modified to include a phase shifter and/or frequency divider in the feedback loop to improve the circuit performance further, which can easily adjust the locking bandwidth and dynamic range of the circuits. Such circuits show promises for constructing high-performance coupled-oscillator arrays, and can be applied in many components and subsystems of communication electronics, such as the frequency synthesizer, FM demodulator, and so on. In the future, we hope to investigate various modifications and applications of the ILPLL, and the noise properties of the PD (or mixer) function of the oscillator in order to further improve the circuit performance and output phase-noise reduction at the low-noise offset frequency.

ACKNOWLEDGMENT

The authors appreciate the support of NEC Corporation, Los Angeles, CA, in donating the GaAs MESFET's, and the Rogers Corporation, Chandler, AZ, in donating the Duroid substrates used in this work. The authors also appreciate X. Cao and this paper's reviewers for helpful suggestions.

REFERENCES

- [1] K. Kurokawa, "Injection locking of microwave solid-state oscillators," *Proc. IEEE*, vol. 61, pp. 1386–1410, Oct. 1973.
- [2] R. A. York, "Nonlinear analysis of phase relationships in quasi-optical oscillator arrays," *IEEE Trans. Microwave Theory Tech.*, vol. 41, pp. 1799–1809, Oct. 1993.
- [3] P. Liao and R. A. York, "A new phase-shifterless beam-scanning technique using arrays of coupled oscillators," *IEEE Trans. Microwave Theory and Tech.*, vol. 41, pp. 1810–1815, Oct. 1993.
- [4] H.-C. Chang and R. A. York, "Enhanced MESFET VCO injection locking bandwidth using low frequency feedback techniques," in *IEEE MTT-S Int. Microwave Symp. Dig.*, San Francisco, CA, June 1996, pp. 1515–1518.

- [5] P. R. Gray and R. G. Meyer, *Analysis and Design of Analog Integrated Circuits*, 2nd Ed. New York: Wiley, 1984, ch. 10.
- [6] H.-C. Chang, X. Cao, U. K. Mishra, and R. A. York, "Phase noise in coupled oscillators: Theory and experiment," *IEEE Trans. Microwave Theory Tech.*, vol. 45, pp. 604–615, May 1997.
- [7] H.-C. Chang, E. S. Shapiro, and R. A. York, "Influence of the oscillator equivalent circuit on the stable modes of parallel-coupled oscillators," *IEEE Trans. Microwave Theory Tech.*, vol. 45, pp. 1232–1239, Aug. 1997.
- [8] H.-C. Chang, X. Cao, M. J. Vaughan, U. K. Mishra, and R. A. York, "Phase noise in externally injection-locked oscillator arrays," *IEEE Trans. Microwave Theory Tech.*, vol. 45, pp. 2035–2042, Nov. 1997.
- [9] H.-C. Chang, X. Cao, U. K. Mishra, and R. A. York, "Phase noise in coupled oscillator arrays," in *IEEE MTT-S Int. Microwave Symp. Dig.*, vol. 2, Denver, CO, June 1997, pp. 1061–1064.
- [10] H.-C. Chang, "Noise and stability analysis of coupled oscillators," Ph.D. dissertation, Dept. Elect. Comput. Eng., Univ. California at Santa Barbara, Santa Barbara, CA, 1998.
- [11] J. J. Lynch, H.-C. Chang, and R. A. York, "Coupled oscillator arrays and scanning techniques" in *Active and Quasi-Optical Arrays for Solid-State Power Combining*, R. A. York and Z. B. Popović, Eds. New York: Wiley, 1997, pp. 135–186.
- [12] R. T. Ramos, P. Gallion, D. Erasme, A. J. Seeds, and A. Bordonalli, "Optical injection locking and phase-lock loop combined systems," *Opt. Lett.*, vol. 19, no. 1, pp. 4–6, Jan. 1994.
- [13] R. T. Ramos and A. J. Seeds, "Comparison between first-order and second-order optical phase-lock loops," *IEEE Microwave Guided Wave Lett.*, vol. 4, pp. 6–8, Jan. 1994.
- [14] B. Skjoldstrup, E. Bodtker, and G. Jacobsen, "New method for electrical frequency locking of optical FDM transmitter," *J. Lightwave Technol.*, vol. 9, pp. 494–504, Apr. 1991.



Heng-Chia Chang (S'95–M'98) received the B.S. degree in electrical engineering from the National Taiwan University, Taipei, Taiwan, R.O.C., in 1990, and M.S. and Ph.D. degrees from the University of California at Santa Barbara, in 1994 and 1998, respectively.

From 1990 to 1992, he served in the Air Force as a Technical Officer in Taiwan, R.O.C. He also received maintenance training in various wireless communication systems, ground control approach (GCA) radar system, digital fiber-optical communication system, and digital private branch exchange (PBX) systems. He is currently a Research Engineer at Santa Barbara Photonics Inc., Santa Barbara, CA. His current research interests include noise analysis, nonlinear microwave-circuit design, coupled-oscillator theory, digital communication system, nonlinear optics, statistical optics, and quantum optics.

Dr. Chang is the member of the IEEE Microwave Theory and Techniques Society (MTT-S).

Andrea Borgioli received the Laurea (Doctor) degree in electronics engineering (*summa cum laude*) from the University of Florence, Florence, Italy, in 1996.

In 1995, he was a Visiting Scholar at the Radiation Laboratory, The University of Michigan at Ann Arbor. In 1997, he joined the Jet Propulsion Laboratory, Pasadena, CA, as a Member of the Technical Staff. Since August 1998, he has been with the University of California at Santa Barbara, as Research Engineer, where he has been involved into various research activities, mainly in the field of the analytical and numerical techniques for applied electromagnetics. His current research interests includes traveling-wave scanning array systems, coupled-oscillator systems, electromagnetic modeling, microelectromechanical (MEMS) devices, and fabrication.

Dr. Borgioli is a member of the Italian Electrical and Electronic Association. He was awarded a Research Fellowship from the University of Florence in 1996.



Pochi Yeh (M'78–SM'87–F'91) received the Ph.D. degree in physics from the California Institute of Technology, Pasadena, CA, in 1977, for research on nonlinear optics and optical properties of superlattices.

He is currently a Professor of electrical and computer engineering at in the Department of Electrical and Computer Engineering (ECE), University of California at Santa Barbara (UCSB). Before he joined UCSB in 1989, he was the Principal Scientist in the Optics Department, Rockwell International

Science Center, Thousand Oaks, CA, where he carried out research in the areas of electrooptics, nonlinear optics, optical phase conjugation, and optical computing. He is known for several important contributions in optics, including the development of a matrix method for optics of layered media, the theory of photorefractive phase conjugators, and the theory of wave mixing in nonlinear media. He has authored or co-authored over 300 journal papers, conference papers, and *Optical Waves in Crystals* (New York: Wiley, 1984), *Optical Waves in Layered Media* (New York: Wiley, 1988), and *Introduction to Photorefractive Nonlinear Optics* (New York: Wiley, 1993).

Dr. Yeh is a Fellow of the Optical Society of America, and the Photonics Society of Chinese-Americans. He was named "Engineer of the Year" by Rockwell Science Center. He received the 1985 Leonardo da Vinci Award. He was also the recipient of the 1989 Rudolf Kingslake Medal and Prize presented by the International Optical Engineering Society.



Robert A. York (S'85–M'89–SM'99) received the B.S. degree in electrical engineering from the University of New Hampshire, Durham, in 1987, and the M.S. and Ph.D. degrees in electrical engineering from Cornell University, Ithaca, NY, in 1989 and 1991, respectively.

He is currently an Associate Professor in the Electrical and Computer Engineering Department, University of California at Santa Barbara (UCSB), where his group is currently involved with the design and fabrication of novel microwave and millimeter-wave circuits, microwave photonics, high-power microwave and millimeter-wave modules using spatial combining and wide-bandgap semiconductor devices, and application of ferroelectric materials to microwave and millimeter-wave circuits and systems.

Dr. York received the 1993 Army Research Office Young Investigator Award and the 1996 Office of Naval Research Young Investigator Award.